SUPPLEMENTARY DATA

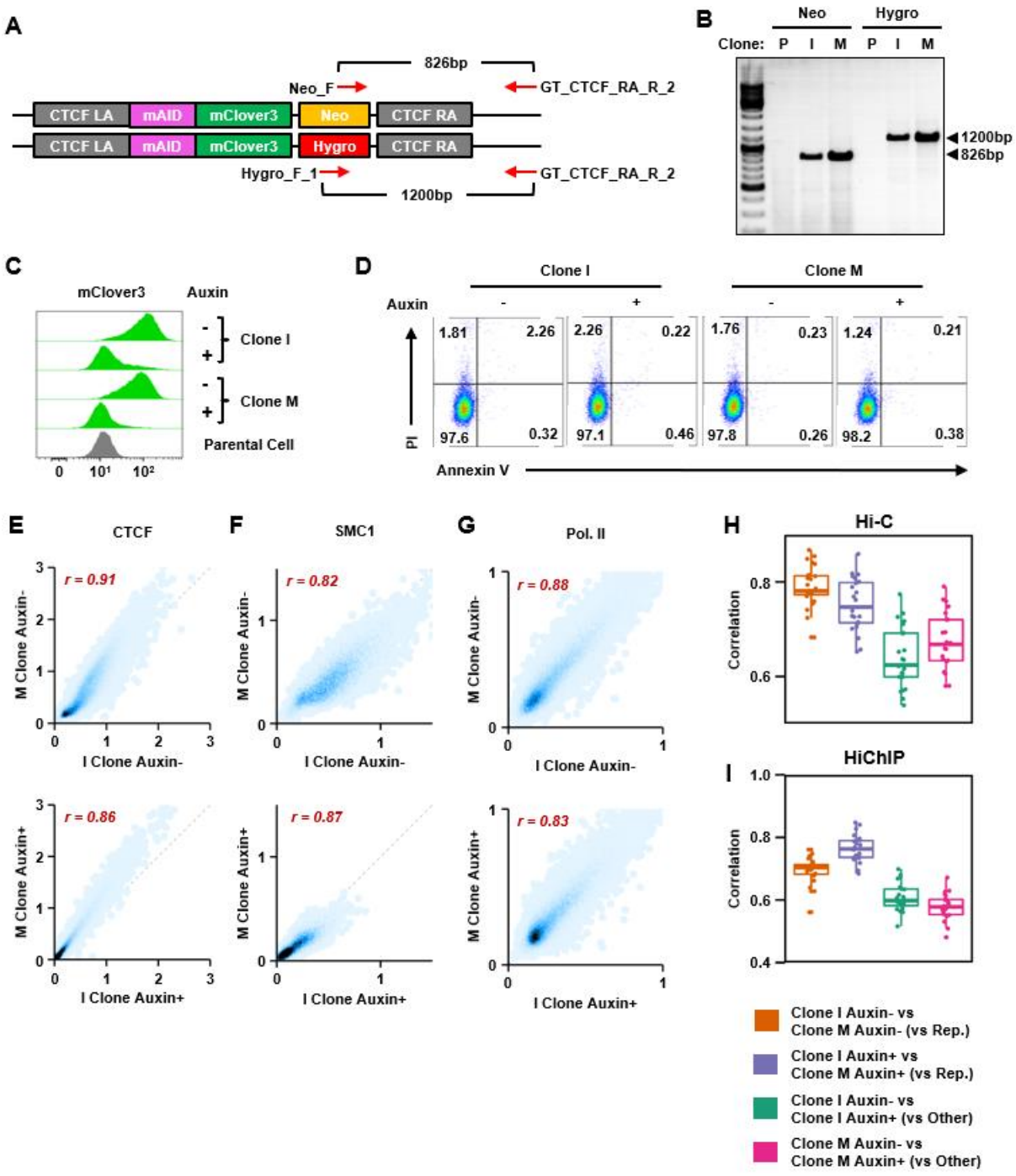

Supplementary Figure S1

(A) Schematic diagram of genotyping by PCR to identify successful knock-in of the mAID-mClover3 cassette to the C-terminus of human *CTCF* before the stop codon in both alleles of

HCT116 cells. Primer sets and expected PCR products are shown. **(B)** Genomic PCR to test the genotype of I and M clones after selection with both G418 and hygromycin. P: Parental cells (HCT116/CMV-OsTIR1). **(C)** Flow cytometric analysis for mClover3 to determine the degradation efficiency of the CTCF-mAID-mClover3 fusion protein upon auxin treatment. Parental cells: HCT116/CMV-OsTIR1. **(D)** Flow cytometric analysis for apoptosis of I and M clones with or without auxin treatment. **(E-G)** Scatter plots show correlations for ChIP-seq signals for (E) CTCF, (F) SMC1, and (G) Pol II between biological replicate cells with (bottom) and without (top) auxin treatment. **(H-I)** Reproducibility analysis of (H) Hi-C and (I) Pol II-HiChIP data in each biological replicate (N=2). Each dot represents a reproducibility score for one chromosome.

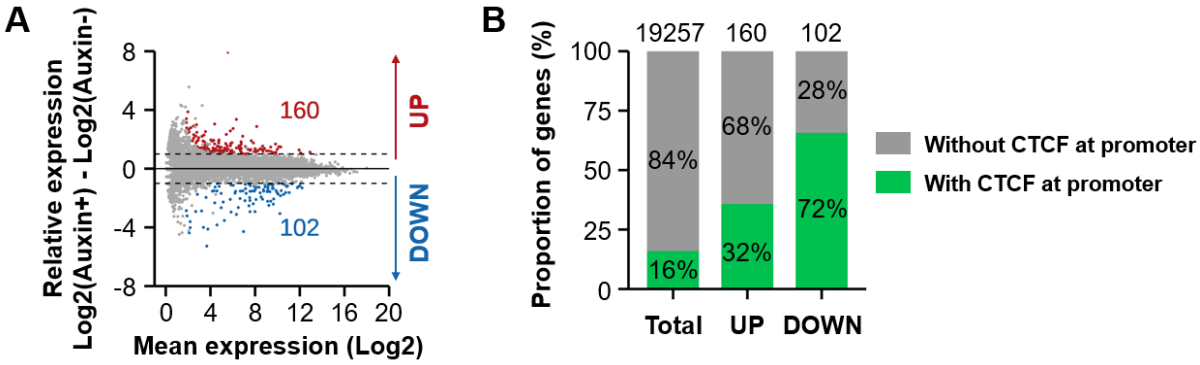

Supplementary Figure S2

(A) RNA-seq MA plot of untreated versus CTCF-depleted cells. The number of genes exhibiting >2-fold increases (red) or decreases (blue) among CTCF-depleted cells with a false discovery rate <0.01 is indicated. **(B)** Proportion of genes with (green) or without (gray) CTCF bound within 2 kb of the transcription start site prior to depletion. The number of genes for each group is listed on top of the bars.

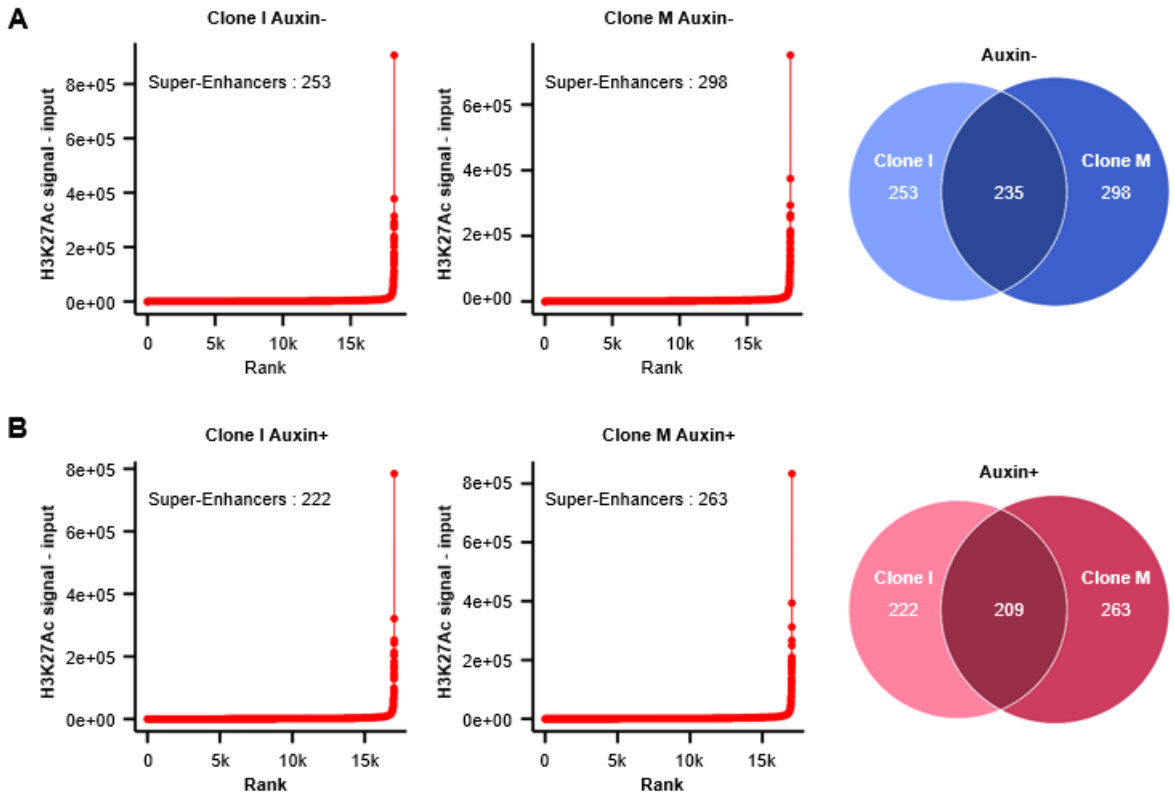

Supplementary Figure S3

Line graphs presenting the number of super-enhancers according to ranked H3K27ac occupancy signals in individual biological replicates **(A)** without and **(B)** with auxin treatment. super-enhancers called from both replicates in each condition were used for subsequent analysis.

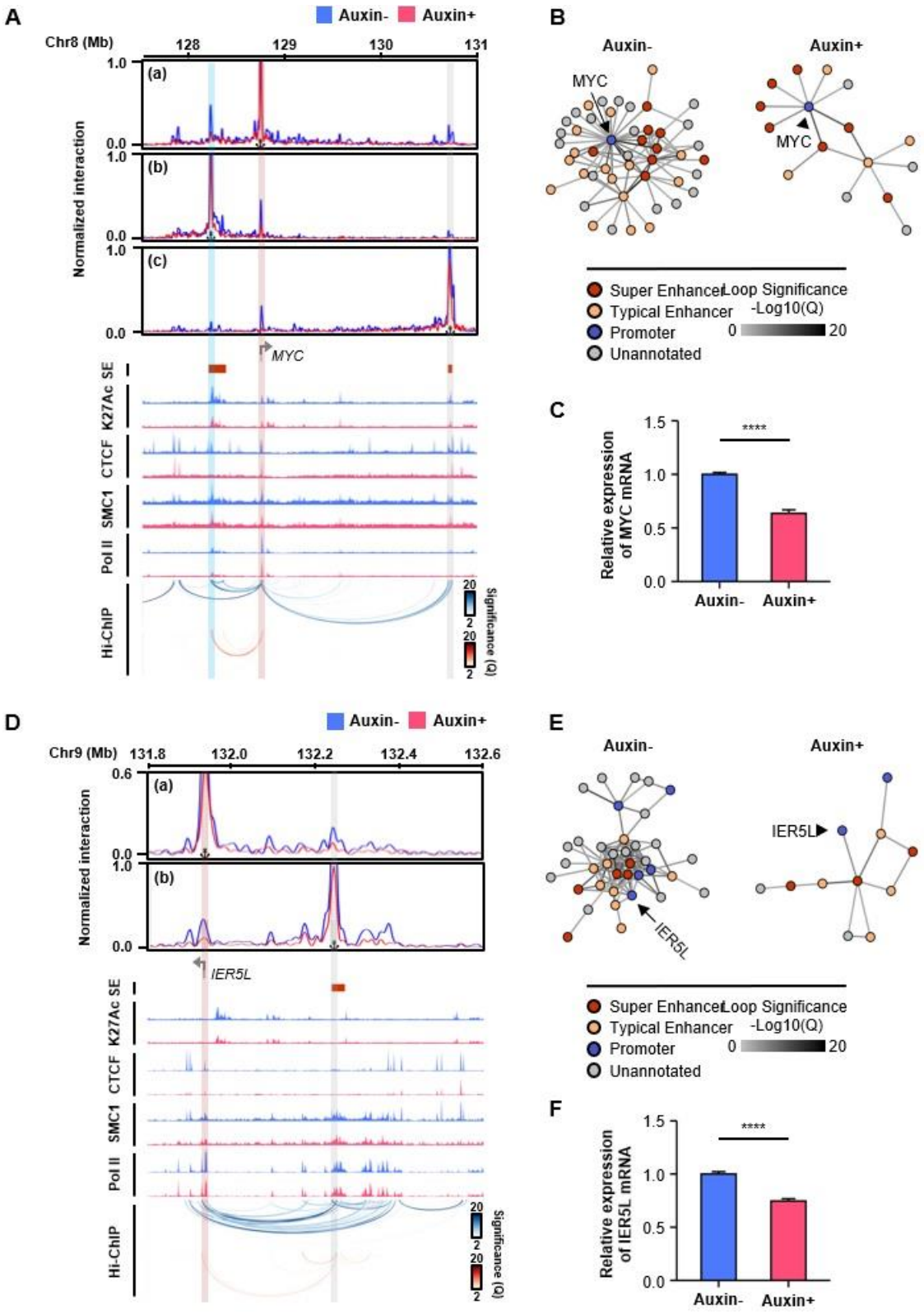

Supplementary Figure S4

(A and D) Snapshots of virtual 4C plots, ChIP-seq signal tracks, and Pol II HiChIP loops (from

top to bottom) at *MYC* (A) and *IER5L* (D) loci with and without auxin treatment. Virtual 4C plots show normalized Pol II HiChIP loop strength with the transcription start site (a), proximal super-enhancer (b), and distal super-enhancer (c) as viewpoints. The locations of super-enhancers are shown on top of H3K27ac ChIP-seq signal tracks. The locations of TAD boundaries are shown on top of Pol II HiChIP loops. Orange vertical bars highlight the locations of the viewpoints at the transcription start site. Sky and gray vertical bars highlight the locations of the viewpoints at super-enhancers. **(B and E)** 3D cliques in the *MYC* (B) and *IER5L* (E) loci, wherein each edge represents a significant Pol II-mediated chromatin interaction. The color of each edge indicates loop strength (-Log10(Q)). The color of each node represents promoter, typical enhancer, super-enhancer, or unannotated regions. **(C and F)** Decreased mRNA expression of *MYC* (C) and *IER5L* (F) upon CTCF depletion was validated with qRT-PCR.

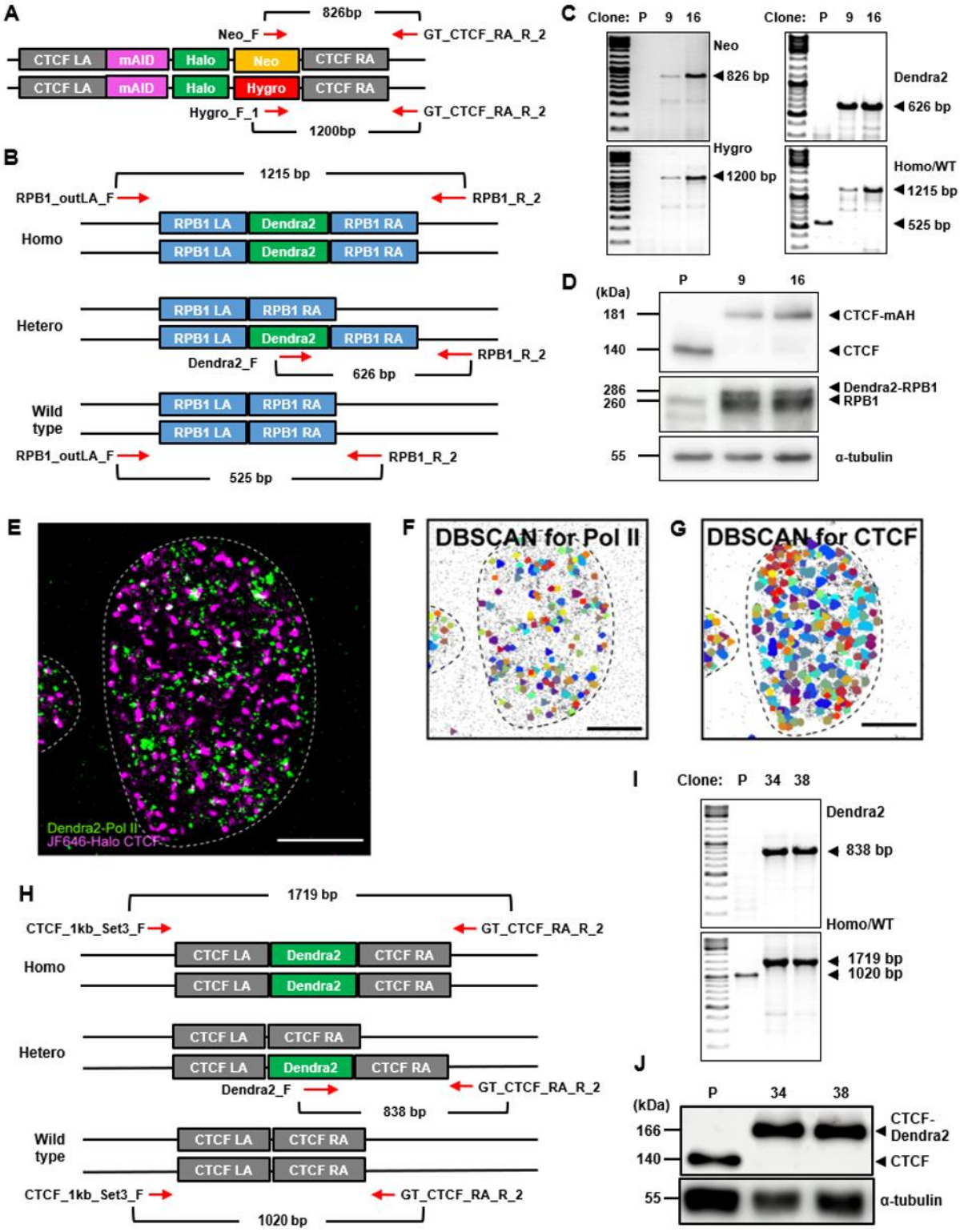

Supplementary Figure S5

(A) Schematic diagram of genotyping by PCR to identify successful knock-in of the mAID-Halo cassette to the C-terminus of human *CTCF* before the stop codon in both alleles of

HCT116 cells. Primer sets and expected PCR products are shown. **(B)** Schematic diagram of genotyping by PCR to identify successful knock-in of Dendra2 to the N-terminus of human *RPB1* before the start codon in both alleles of HCT116 cells. Primer sets and expected PCR products are shown. **(C)** Genomic PCR to test the genotype of clones after selection. P: Parental cells (HCT116/CMV-OsTIR1). **(D)** Immunoblotting analysis for CTCF and RPB1 to identify the CTCF-mAID-Halo (CTCF-mAH) and Dendra2-RPB1 fusion protein. Parental cells: HCT116/CMV-OsTIR1. **(E)** A super-resolved merged image of JF646-CTCF (magenta) and Dendra2-Pol II (green). From localization of individual fluorescence, **(F)** Pol II clusters and **(G)** CTCF clusters were defined using the DBSCAN algorithm. Scale bars represent 5 μm. **(H)** Schematic diagram of genotyping by PCR to identify successful knock-in of Dendra2 to the C-terminus of human *CTCF* before the stop codon in both alleles of HCT116 cells. Primer sets and expected PCR products are shown. **(I)** Genomic PCR to test the genotype of clones after selection. P: Parental cells (HCT116/CMV-OsTIR1). **(J)** Immunoblotting analysis for CTCF to identify the CTCF-Dendra2 fusion protein. Parental cells: HCT116/CMV-OsTIR1.

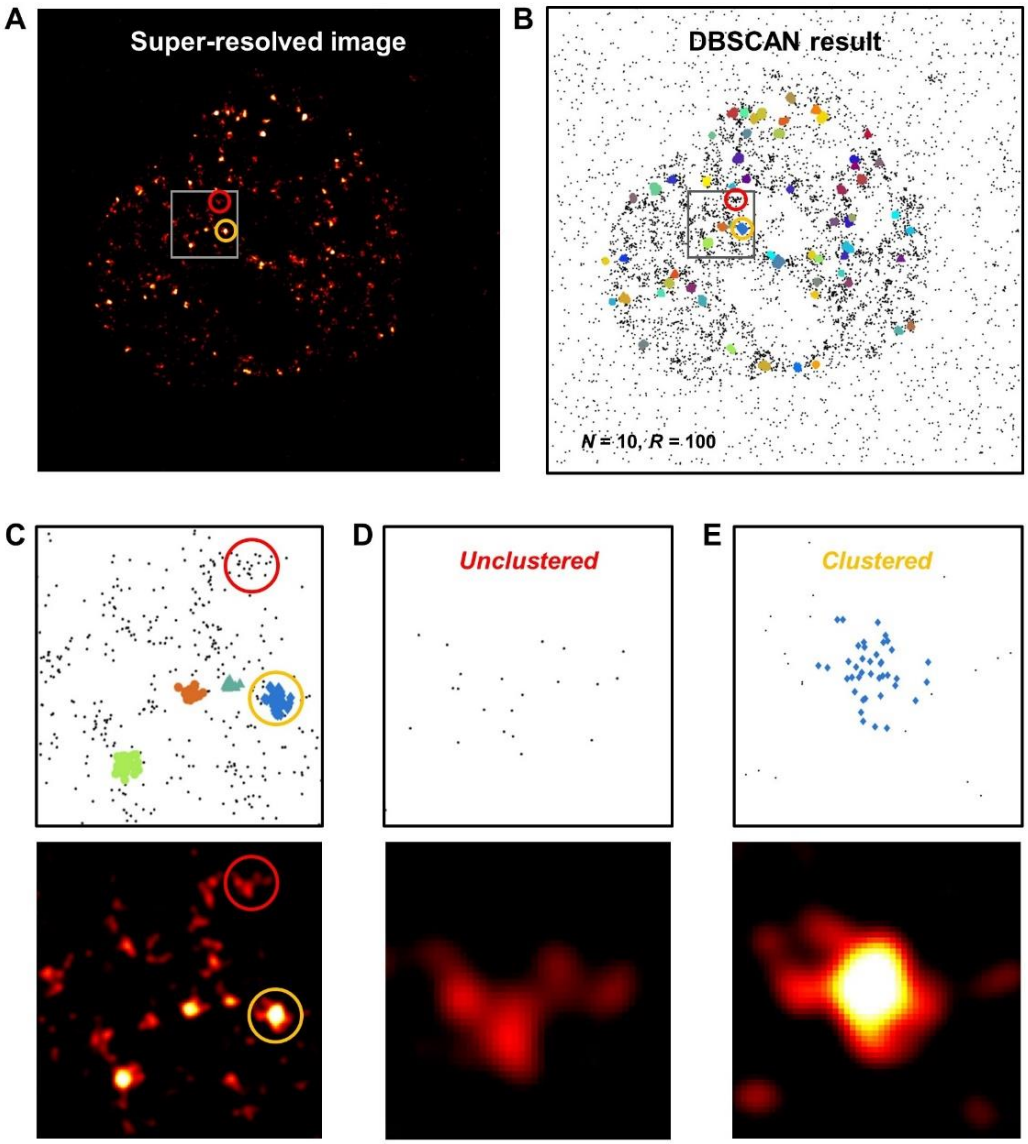

Supplementary Figure S6

(A and B) Representative super-resolved color code image (A) and the pointillist image (B) for Dendra2-Pol II where localization-dense regions defined as “unclustered” and “clustered” were indicated with red and yellow circles, respectively. (C – E) Progressively zoomed-in pointillist image (top) and super-resolved color code image (bottom) for Dendra2-Pol II. (C) Zoomed-in images for the gray box of panel B. (D and E) Zoomed-in images for the red (D) and yellow (E) circles of panel C. Estimation by DBSCAN with N = 10 and R = 100 nm shows 71 Pol II clusters at this 2D focal plane.

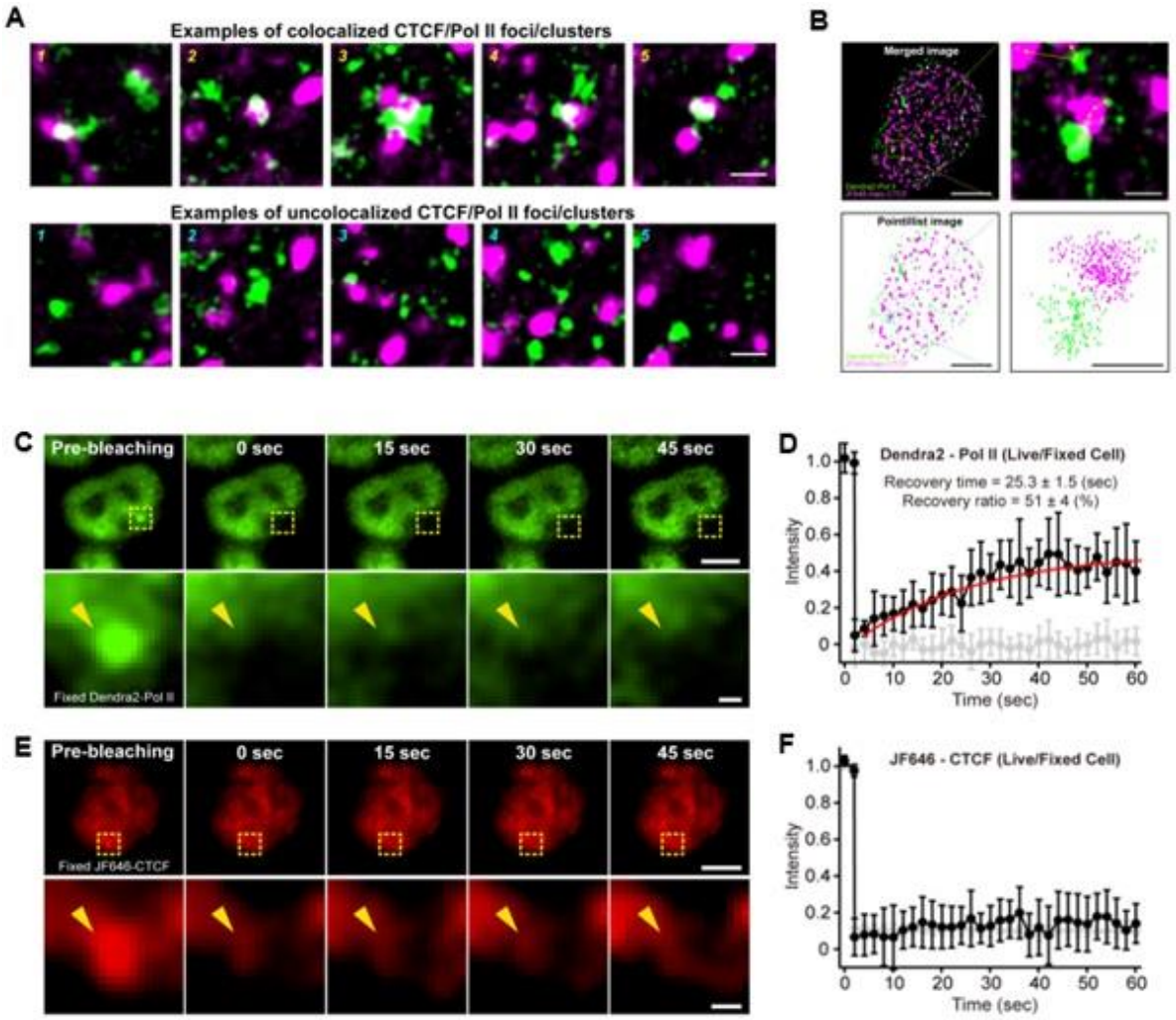

Supplementary Figure S7

(A) Examples of colocalized and un-colocalized CTCF/Pol II clusters. **(B)** Analysis of center-to-center distances between CTCF/Pol II clusters defined using the DBSCAN algorithm. A representative merged super-resolved image shows (magenta) JF646-CTCF and (green) Dendra2-Pol II clusters in a cell nucleus. The enlarged image shows the region demarcated by the dotted box drawn in the merged image. Yellow arrows represent the distance between adjacent CTCF and Pol II clusters. Pointillist images represent localizations of stochastic fluorescent signals. **(C)** An example of the FRAP experiment for a Pol II cluster in a fixed cell at 15-sec intervals. The yellow dotted box indicates a photobleached region in the upper panel. Fluorescence of bleached Pol II clusters did not recover in fixed cells, unlike live cells. **(D)**

Normalized fluorescence intensities over time for Pol II clusters in live cells (black) and fixed cells (grey) during FRAP experiments. **(E)** An example of the FRAP experiment for a CTCF cluster in a fixed cell at 15-sec intervals. **(F)** Normalized fluorescence intensities over time for CTCF clusters in live cells (black) and fixed cells (grey) during FRAP experiments. Fluorescence of bleached CTCF clusters did not recover in either fixed or live cells. Scale bars represent 5 μm (upper panels) and 500 nm (lower panels).

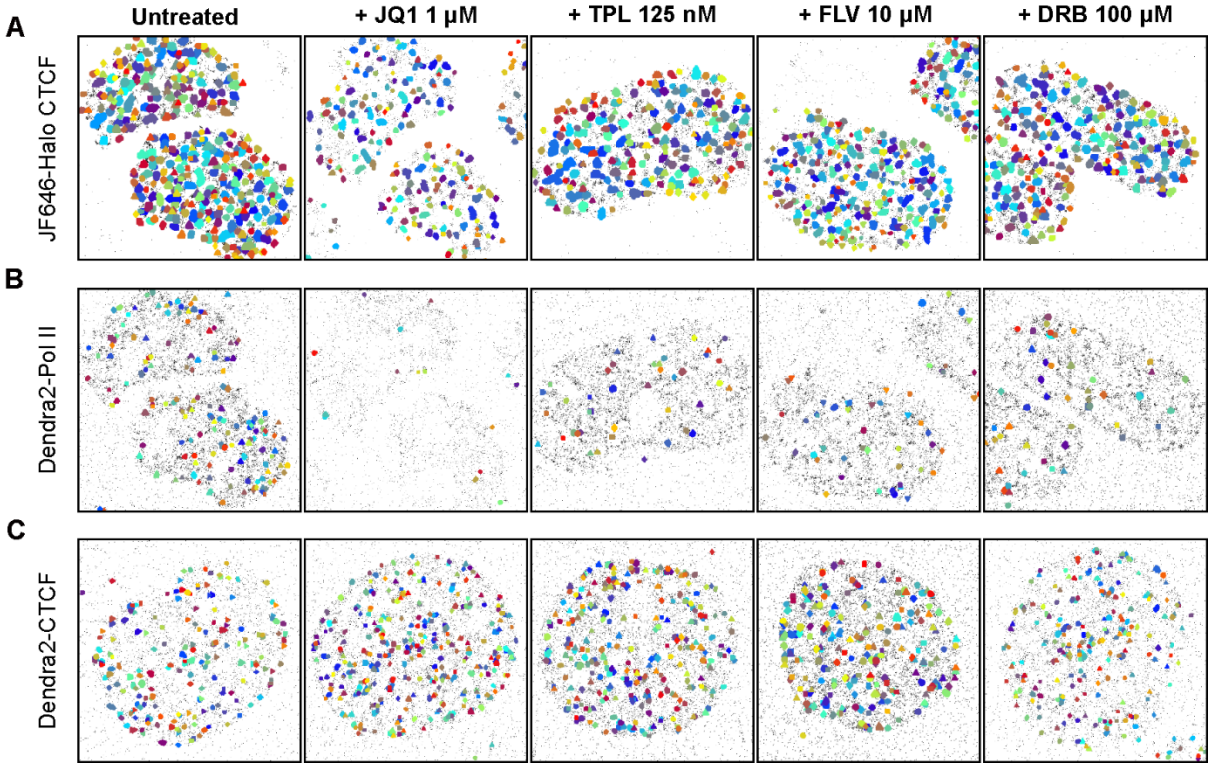

Supplementary Figure S8

Representative DBSCAN results of **(A)** JF646-Halo-CTCF, **(B)** Dendra2-Pol II clusters, and **(C)** Dendra2-CTCF in cell nuclei before and after treatment with JQ1 (1 μM, 2 hr), triptolide (TPL; 125 nM, 2 hr), flavopiridol (FLV; 10 μM, 2 hr), and DRB (100 μM, 2 hr). The matched super-resolved color code images are shown in Figure 5A and 5B.

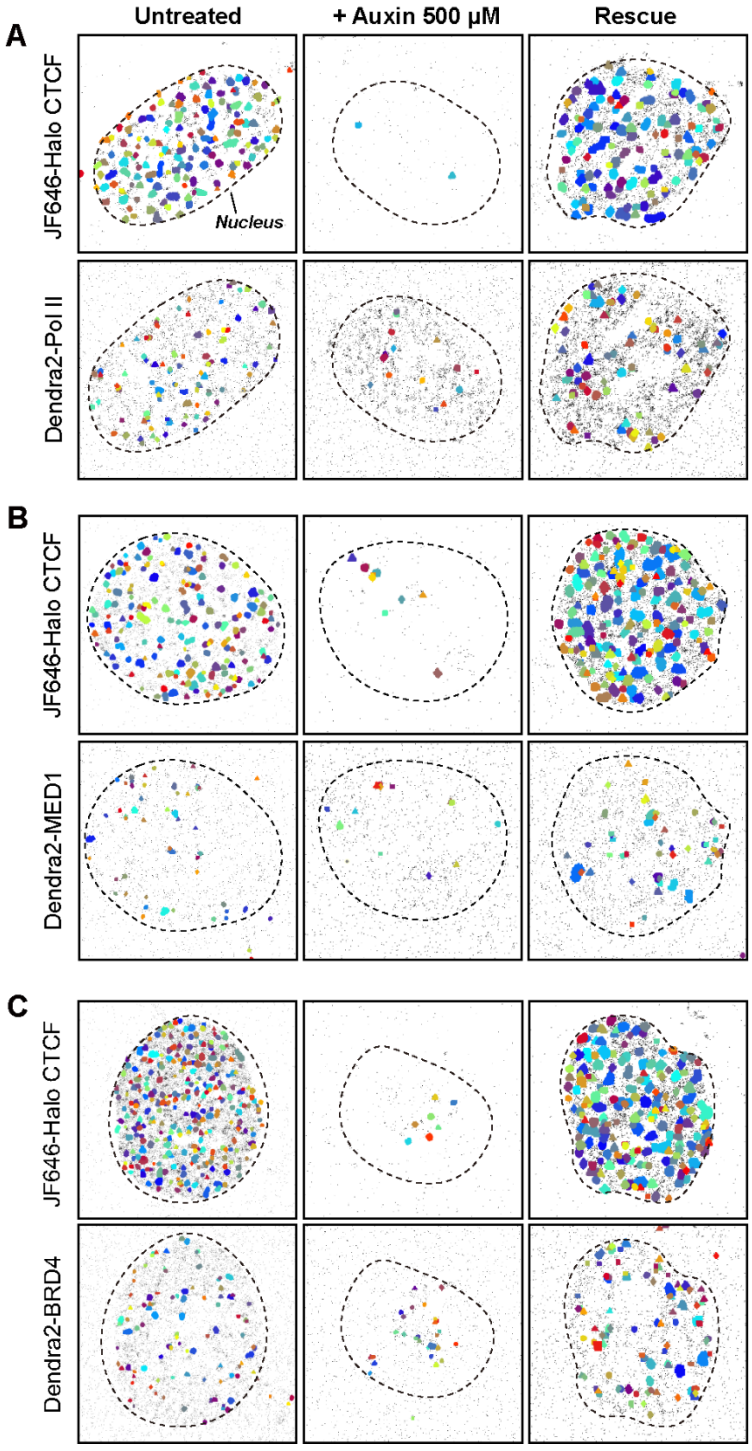

Supplementary Figure S9

Representative DBSCAN results of JF646-Halo-CTCF/Dendra2-Pol II cells **(A),** JF646-Halo-CTCF/Dendra2-MED1 cells **(B)**, and JF646-Halo-CTCF/Dendra2-BRD4 cells **(C)** before and

after auxin treatment. The matched super-resolved color code images are shown in Figure 6B, 6F, and 6J, respectively.

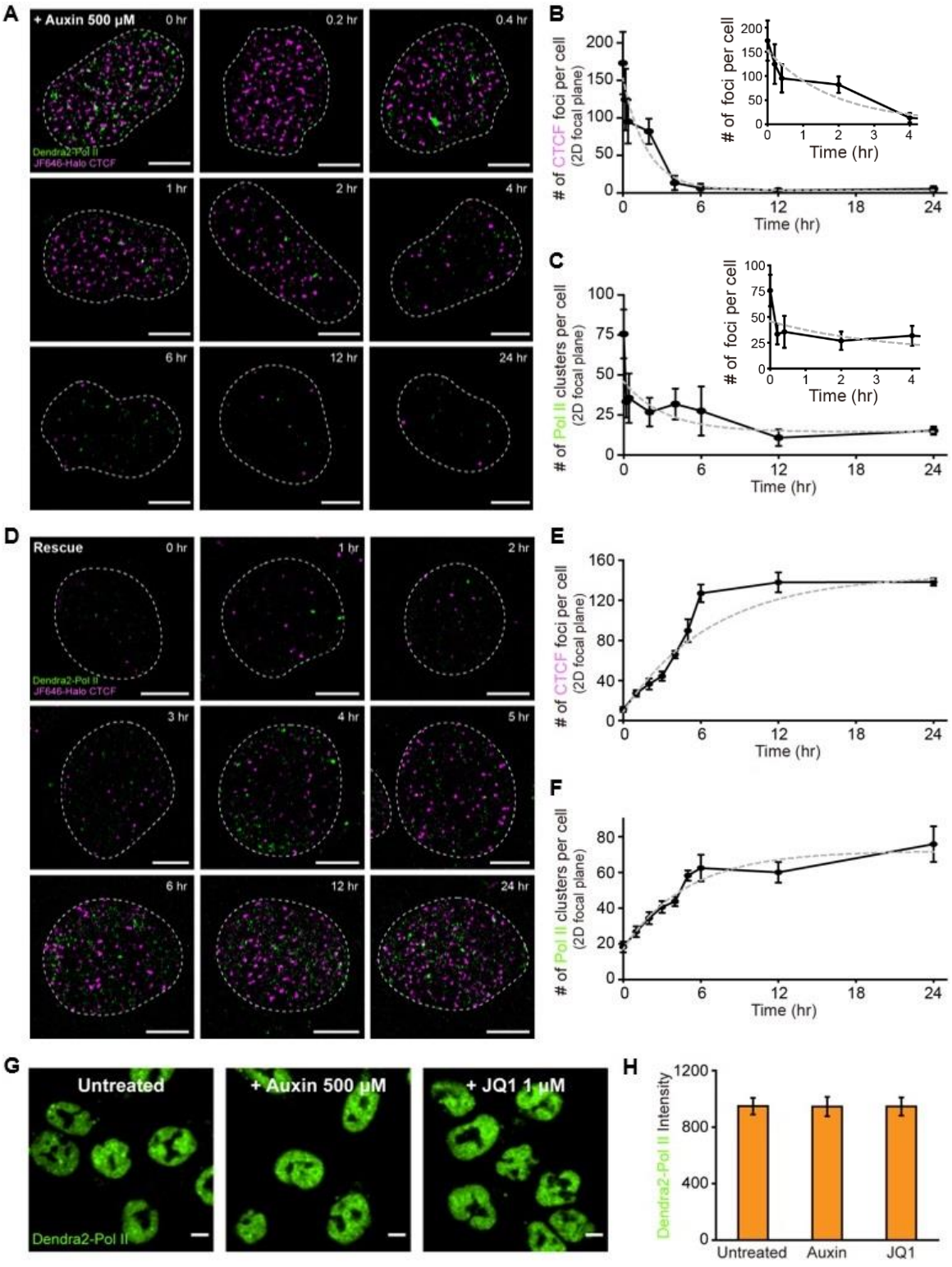

Supplementary Figure S10

(A) Representative super-resolved images of JF646-CTCF (magenta) and Dendra2-Pol II (green) clusters per cell over time after auxin treatment. **(B and C)** Time course curves for

number of (B) CTCF clusters and (C) Pol II clusters per cell after auxin treatment. Insets represent rapid decreases in the number of clusters until 4 hours after auxin treatment. **(D)** Representative super-resolved images of JF646-CTCF (magenta) and Dendra2-Pol II (green) clusters over time after auxin removal. **(E and F)** Time course curves for number of (E) CTCF clusters and (F) Pol II clusters per cell after auxin removal. $N = 11.6$ (±1.2) cells were analyzed for each time point for line graphs. **(G)** Representative fluorescence images of the Halo-CTCF/Dendra2-Pol II cell line upon excitation with a 488-nm laser. Fluorescence signals in nuclei indicate expression of Dendra2-Pol II in (left) untreated cells, (middle) auxin-treated cells (500 μM for 24 hr), and (right) JQ1-treated cells (1 μM for 2 hr). **(H)** Comparison of fluorescence intensities of nuclei among untreated, auxin-treated, and JQ1-treated cells. The intensities in the y-axis are arbitrary numbers. All scale bars represent 5 μm.

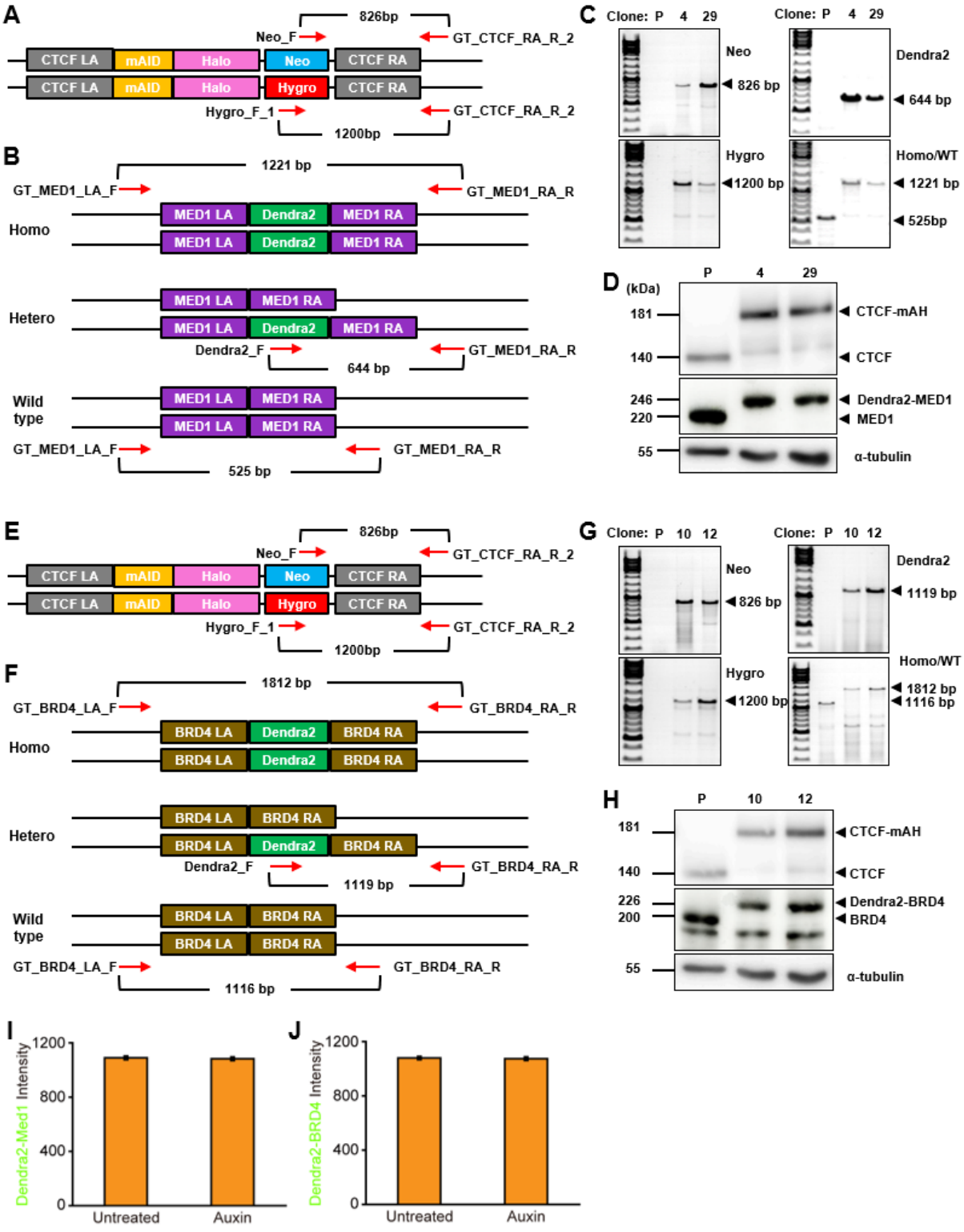

Supplementary Figure S11

(A) Schematic diagram of genotyping by PCR to identify successful knock-in of the mAID-Halo cassette to the C-terminus of human *CTCF* before the stop codon in both alleles of

HCT116 cells. Primer sets and expected PCR products are shown. **(B)** Schematic diagram of genotyping by PCR to identify successful knock-in of Dendra2 to the N-terminus of human *MED1* before the start codon in both alleles of HCT116 cells. Primer sets and expected PCR products are shown. **(C)** Genomic PCR to test the genotype of clones after selection. P: Parental cells (HCT116/CMV-OsTIR1). **(D)** Immunoblotting analysis for CTCF and MED1 to identify the CTCF-mAID-Halo (CTCF-mAH) and Dendra2-MED1 fusion protein. Parental cells: HCT116/CMV-OsTIR1. **(E)** Schematic diagram of genotyping by PCR to identify successful knock-in of the mAID-Halo cassette to the C-terminus of human *CTCF* before the stop codon in both alleles of HCT116 cells. Primer sets and expected PCR products are shown. **(F)** Schematic diagram of genotyping by PCR to identify successful knock-in of Dendra2 to the N-terminus of human *BRD4* before the start codon in both alleles of HCT116 cells. Primer sets and expected PCR products are shown. **(G)** Genomic PCR to test the genotype of clones after selection. P: Parental cells (HCT116/CMV-OsTIR1). **(H)** Immunoblotting analysis for CTCF and BRD4 to identify the CTCF-mAID-Halo (CTCF-mAH) and Dendra2-BRD4 fusion protein. Parental cells: HCT116/CMV-OsTIR1. **(I-J)** Fluorescence intensities in cell nuclei for (I) Dendra2-MED1 and (J) Dendra2-BRD4 before and after auxin treatment (500 μM for 24 hr) upon excitation with a 488-nm laser. The intensities in the y-axis are arbitrary numbers.

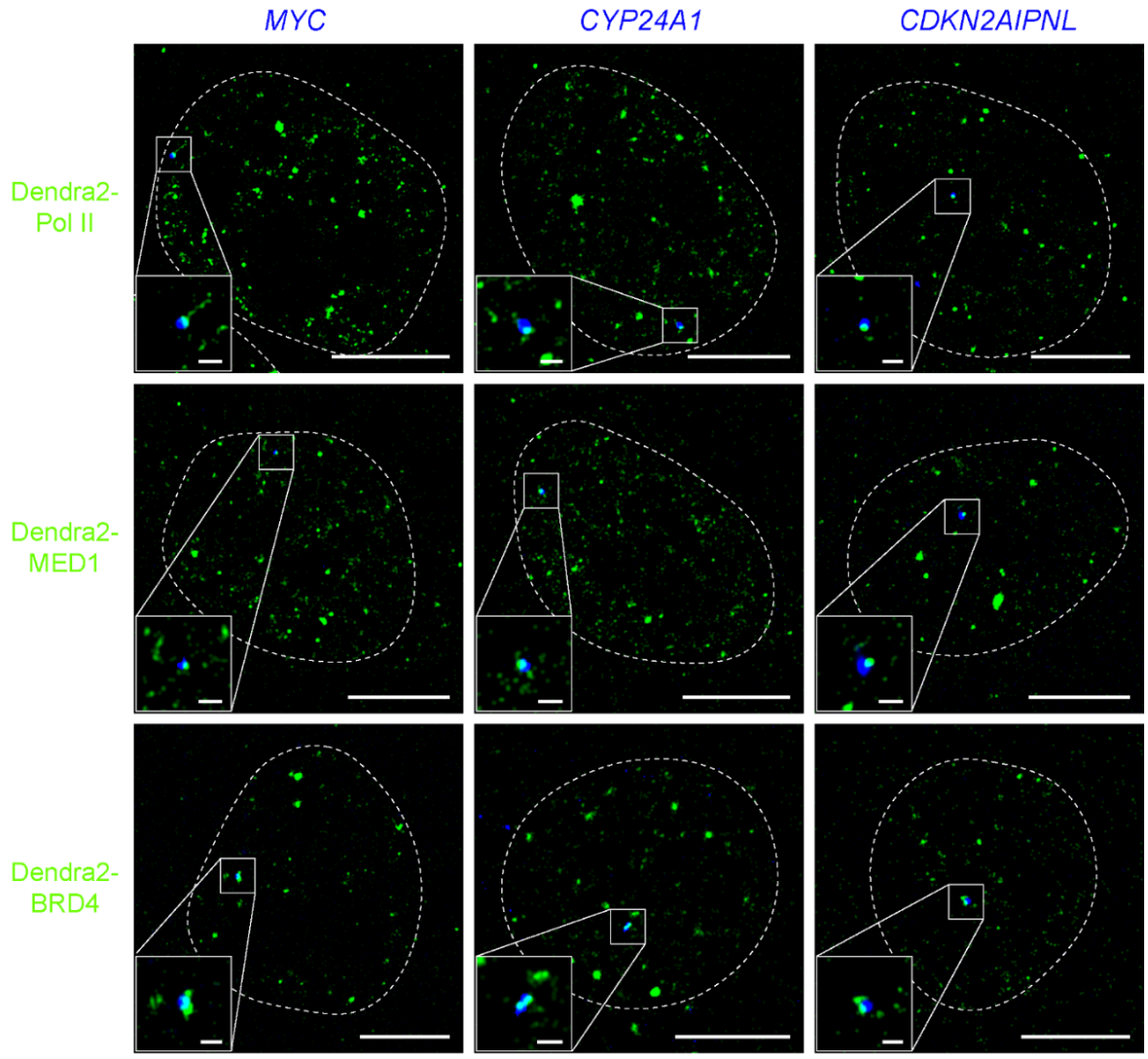

Supplementary Figure S12

Representative super-resolved colocalization images to address transcriptional condensates associated with active genes. RNA FISH was used for capturing nascent transcription loci for *MYC*, *CYP24A1*, and *CDKN2AIPNL* genes (left to right). Pol II/BRD4/MED1 clusters were colocalized with the nascent gene loci.

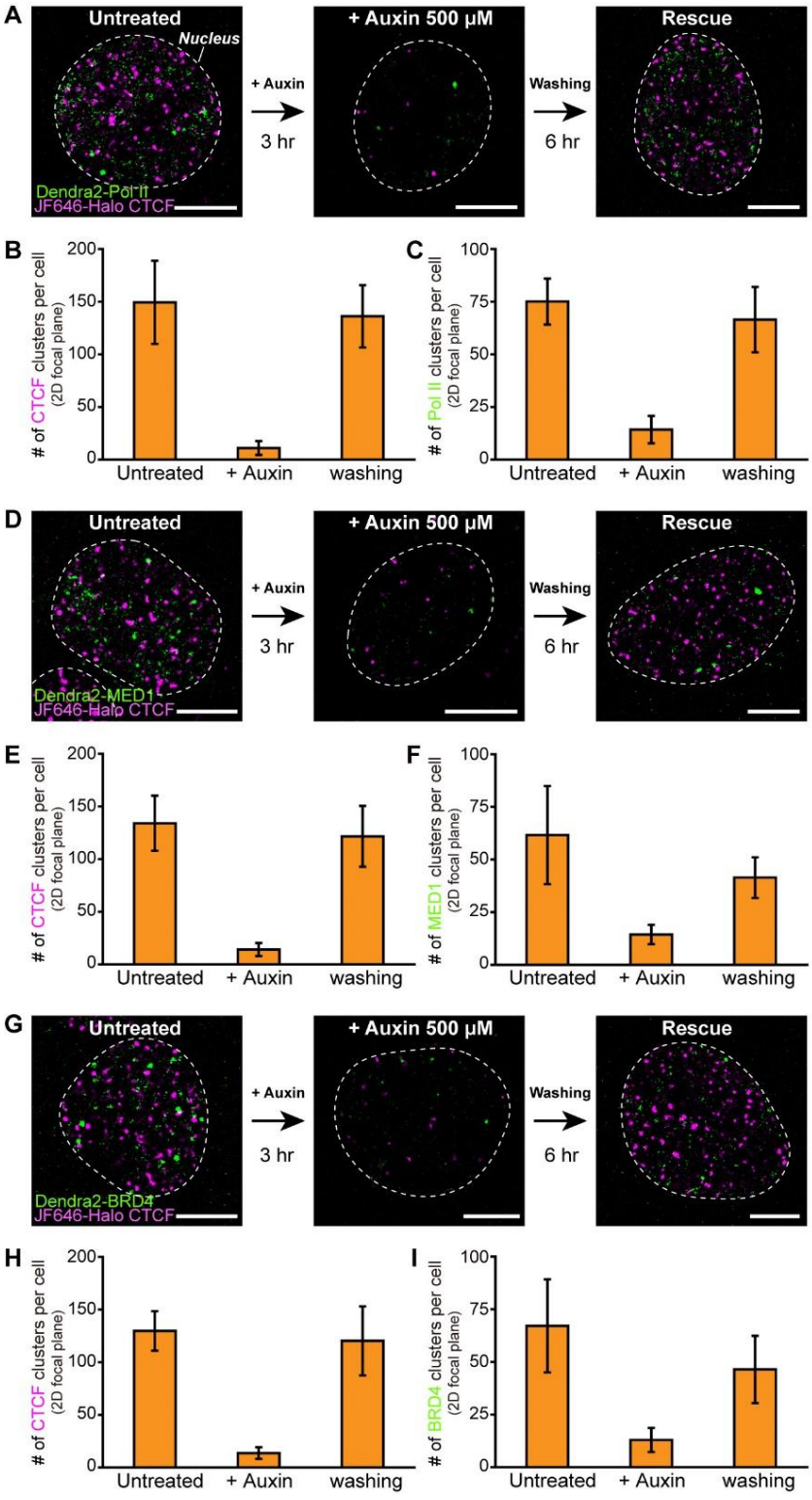

Supplementary Figure S13

(A, D, G) Representative dual-color super-resolved images of (A) Pol II, (D) MED1, and (G) BRD4 clusters, along with CTCF clusters, upon CTCF degradation with 3-hr auxin treatment

and restoration with 6-hr auxin removal. **(B, E, H)** Numbers of CTCF clusters per cell per 2D-focal plane for each cell line. **(C, F, I)** Numbers of (C) Pol II, (F) MED1, and (I) BRD4 clusters per cell per 2D-focal plane upon CTCF degradation and restoration. Auxin (500 μM) was treated for 3 hr for CTCF degradation and washed out for 6 hr for CTCF restoration. The results are consistent with degradation and restoration for 24 hrs (**Figure 6**). Scale bars represent 5 μm. N = 18 (±3.4) cells, in average, were analyzed for each cell line.

Table S1. List of oligonucleotides used in the study

Primers used for amplification of gene construct		
Name	**Description**	**Sequence (5'-3')**
CTCF_500bp_F	Amplifying CTCF HR arm from genomic DNA	gaaactagtCTAAAAGACCCTTGTGATTCTTGG
CTCF_500bp_R	Amplifying CTCF HR arm from genomic DNA	gaaggtaccCACTGTCCTCAGCACTTCAC
XhoI_F	Amplifying BRD4 HR arm Gene block	gaaattaacgcacgctcgCT
KpnI_R	Amplifying BRD4 HR arm Gene block	tatgctacgctacgctacgc
SpeI_F	Amplifying MED1 HR arm Gene block	gaaattaacgcacgctcgACT
KpnI_R	Amplifying MED1 HR arm Gene block	tatgctacgctacgctacgc
Halo_F	Amplifying HaloTag	gaagctagcATGGCAGAAATCGGTA
Halo_R	Amplifying HaloTag	gaatctagaGCCGGAAATCTCGAGC
BamHI_Dendra2_F	Amplifying Dendra2 gene	gaaggatccATGAACACCCCG
BamHI_Dendra2_R	Amplifying Dendra2 gene	cttggatccTTACCACACCTGG
Primers used for sgRNAs		
Name	**Description**	**Sequence (5'-3')**
CTCF_sgR_F_02	guide RNA targeting CTCF locus	caccgTCAGCATGATGGACCGGTGA
CTCF_sgR_R_02	guide RNA targeting CTCF locus	aaacTCACCGGTCCATCATGCTGAc
BRD4_sgRNA_F	guide RNA targeting BRD4 locus	caccgTGGGATCACTAGCATGTCTG
BRD4_sgRNA_R	guide RNA targeting BRD4 locus	aaacCAGACATGCTAGTGATCCCAc
MED1_sgRNA_F	guide RNA targeting MED1 locus	caccgCTTCAGGATGAAAGCTCAGG
MED1 sgRNA_R	guide RNA targeting MED1 locus	aaacCCTGAGCTTTCATCCTGAAGc
Primers used for genotyping		
Name	**Description**	**Sequence (5'-3')**
GT_CTCF_RA_R_2	Genotyping	CTCCAAGCAAAGGGAGTCAG
CTCF_1kb_Set3_F	Genotyping	GAAACTAGTTCACCTGAGGTCAGTAGTTCC
RPB1_outLA_F	Genotyping	CCGTAACCTCTGCCGTTCAG
RPB1_R_2	Genotyping	CCTGGCCCGTCACCCATAAG
GT_BRD4_LA_F	Genotyping	GTGGGAAAAGGGATGTGCAG
GT_BRD4_RA_R	Genotyping	GGTGACAGTGACGATGATGC
GT_MED1_LA_F	Genotyping	TTTCGATGCCCTGTCCTCTT
GT_MED1_RA_R	Genotyping	CAAAAGTGCCCTAGTCGAGC
Neo_F	Genotyping	AATGGGCTGACCGCTTCCTC
Hygro_F_1	Genotyping	ACTGTCGGGCGTACACAAAT
Dendra2_F	Genotyping	TGCACCATCCGCAGCGACAT
Primers used for mutagenesis		
Name	**Description**	**Sequence (5'-3')**
CTCF_SB_F_02	Site-directed mutagenesis	GATCCTCtcCATGATGGACCGGgGATccCGGAGCCTTGTGCGTCGCC
CTCF_SB_R_02	Site-directed mutagenesis	GGCGACGCACAAGGCTCCGggATCcCCGGTCCATCATGgaGAGGATC

Primers used for RT-qPCR		
Name	**Description**	**Sequence (5'-3')**
GAPDH_F	qRT-PCR	AGGGCTGCTTTTAACTCTGGT
GAPDH_R	qRT-PCR	CCCCACTTGATTTTGGAGGGA
IRS1_F	qRT-PCR	CTCAACTGGACATCACAGCAG
IRS1_R	qRT-PCR	TGAAATGGATGCATCGTACC
MYC_F	qRT-PCR	CTGCTTAGACGCTGGATTT
MYC_R	qRT-PCR	GTCGTAGTCGAGGTCATAGT
IER5L_F	qRT-PCR	TGGTCAGCTGTGGTGTTTGT
IER5L_R	qRT-PCR	TCTCACAGGCTCGAACAATG

Supplementary Table S2. Summary of Hi-C data used in this study.

	Clone I Auxin-	Clone M Auxin-	Merge Auxin-	Clone I Auxin+	Clone M Auxin+	Merge Auxin+
Total_pairs_processed	216,229,102	234,403,906	450,633,008	228,359,744	245,326,175	473,685,919
Unmapped_pairs	3,240,560	4,519,362	7,759,922	4,609,648	4,831,234	9,440,882
Low_qual_pairs	70,081,835	74,396,373	144,478,208	74,348,409	78,772,354	153,120,763
Unique_paired_alignments	125,267,707	135,638,164	260,905,871	130,566,210	141,130,535	271,696,745
Multiple_pairs_alignments	0	0	0	0	0	0
Pairs_with_singleton	17,639,000	19,850,007	37,489,007	18,835,477	20,592,052	39,427,529
Low_qual_singleton	0	0	0	0	0	0
Unique_singleton_alignments	0	0	0	0	0	0
Multiple_singleton_alignments	0	0	0	0	0	0
Reported_pairs	125,267,707	135,638,164	260,905,871	130,566,210	141,130,535	271,696,745
valid_interaction	103,587,750	104,346,481	207,934,231	100,318,546	107,088,148	207,406,694
valid_interaction_rmdup	92,976,103	86,848,111	179,821,709	85,625,812	90,424,045	176,046,966
trans_interaction	13,402,832	20,209,400	33,612,160	14,178,137	17,316,844	31,494,896
cis_interaction	79,573,271	66,638,711	146,209,549	71,447,675	73,107,201	144,552,070
cis_shortRange	24,103,745	18,146,473	42,248,009	21,102,614	22,106,989	43,206,975
cis_longRange	55,469,526	48,492,238	103,961,540	50,345,061	51,000,212	101,345,095

Supplementary Table S3. Summary of Pol II HiChIP data used in this study.

	Clone I Auxin-	Clone M Auxin-	Merge Auxin-	Clone I Auxin+	Clone M Auxin+	Merge Auxin+
Total_pairs_processed	213,041,509	231,927,353	444,968,862	224,790,327	215,670,701	440,461,028
Unmapped_pairs	6,884,110	3,501,502	10,385,612	3,999,873	3,061,895	7,061,768
Low_qual_pairs	85,874,138	78,321,900	164,196,038	77,784,991	71,041,074	148,826,065
Unique_paired_alignments	105,117,431	132,167,165	237,284,596	126,822,036	127,909,629	254,731,665
Multiple_pairs_alignments	0	0	0	0	0	0
Pairs_with_singleton	15,165,830	17,936,786	33,102,616	16,183,427	13,658,103	29,841,530
Low_qual_singleton	0	0	0	0	0	0
Unique_singleton_alignments	0	0	0	0	0	0
Multiple_singleton_alignments	0	0	0	0	0	0
Reported_pairs	105,117,431	132,167,165	237,284,596	126,822,036	127,909,629	254,731,665
valid_interaction	79,169,952	98,286,511	177,456,463	100,771,751	104,973,964	205,745,715
valid_interaction_rmdup	59,117,595	82,333,628	141,445,796	83,526,840	89,992,877	173,514,102
trans_interaction	8,919,522	12,277,453	21,196,956	11,681,173	13,050,054	24,731,205
cis_interaction	50,198,073	70,056,175	120,248,840	71,845,667	76,942,823	148,782,897
cis_shortRange	18,806,729	29,190,739	47,992,207	24,292,226	24,670,834	48,957,780
cis_longRange	31,391,344	40,865,436	72,256,633	47,553,441	52,271,989	99,825,117

Table S4. Reagents or resources used in this study.

REAGENT or RESOURCE	SOURCE	IDENTIFIER
Antibodies		
Rabbit polyclonal anti-CTCF	CST	Cat# 2899
Rabbit polyclonal anti-SMC1	Bethyl Laboratories	Cat# A300-055A
Rabbit polyclonal anti-H3K27ac	Abcam	Cat# ab4729
Rabbit monoclonal anti-Phospho-Rpb1 CTD	CST	Cat# 13523
Rabbit polyclonal anti-BRD4	Bethyl Laboratories	Cat# A301-985A100
Mouse monoclonal anti-α-Tubulin	Santa Cruz	Cat# sc-32293
Rabbit polyclonal anti-MED1	Bethyl Laboratories	Cat# A300-793A
Mouse monoclonal anti-RPB1	Abcam	Cat# ab5408
HRP-linked anti-Rabbit IgG	CST	Cat# 7074
HRP-linked anti-Mouse IgG	CST	Cat# 7076
Chemicals, Peptides, and Recombinant Proteins		
RPMI 1640, 1X, with 2.05mM L-Glutamine	HyClone	Cat# SH30027.01
Fetal bovine serum	HyClone	Cat# SH30071.03
Penicillin-Streptomycin solution	HyClone	Cat# SV30010
DMEM with HEPES and without phenol red	Gibco	Cat# 21063-029
Fetal bovine serum, Canada Origin	Gibco	Cat# 12483-020
Penicillin-Streptomycin solution	Gibco	Cat# 15140-122
Trypsin-EDTA (0.05%), phenol red	Gibco	Cat# 25300062
Phosphate buffered saline	Gibco	Cat# 10010-023
Leibovitz's L-15 medium, no phenol red	Gibco	Cat# 21083-027
4% Paraformaldehyde solution	Biosesang	Cat# PC2031-050-00
JQ1	Sigma-Aldrich	Cat# SML0974
Triptolide	Sigma-Aldrich	Cat# T3652
Flavopiridol hydrochloride hydrate	Sigma-Aldrich	Cat# F3055
5,6-Dichlroro-1-β-D-ribofuranosyl-benzimidazole	Sigma-Aldrich	Cat# D1916
Dimethyl sulfoxide	Sigma-Aldrich	Cat# D8418
1,6-Hexandiol	Sigma-Aldrich	Cat# 240117
Janelia Fluor® HaloTag® Ligands	Promega	Cat# GA1120
Q5® High-Fidelity DNA Polymerase	New England Biolabs	Cat# M0491L
Hybrid-R™ RNA purification kit	GeneAll Biotechnology	Cat# 305-101
PrimeScript™ RT Master Mix	Takara Bio	Cat# RR036A
QuantiNova™ SYBR® Green PCR Kit	QIAGEN	Cat# 208052
T-PER Tissue Protein Extraction Reagent	Thermo Scientific	Cat# 78510
Halt™ Protease and Phosphatase Inhibitor Cocktail	Thermo Scientific	Cat# 78440
Protein Assay Dye Reagent Concentrate	Bio-Rad	Cat# 5000006
Pierce™ ECL Western Blotting Substrate	Thermo Scientific	Cat# 32106
Pierce™ ECL Plus Western Blotting Substrate	Thermo Scientific	Cat# 32132
Supersignal™ West Femto Maximum Sensitivity Substrate	Thermo Scientific	Cat# 34096
Annexin Ⅴ Apoptosis Detection Kit	eBioscience	Cat# 88-8007-74
formaldehyde solution	Sigma	Cat# F8775
Dynabeads™ protein A	Invitrogen	Cat# 100.02D
Dynabeads™ protein G	Invitrogen	Cat# 100.04D
Proteinase K, Molecular Biology Grade	New England Biolabs	Cat# P8107S

AMPure XP	Beckman Coulter	Cat# A63881
Nextera DNA Library Preparation Kit	illumina	Cat# 15028212
KAPA HiFi HotStart ReadyMix PCR Kit	KAPA Biosystems	Cat# KK2602
DpnⅡ	New England Biolabs	Cat# R0543
NEBuffer3.1	New England Biolabs	Cat# B7203S
biotin-14-dATP	Jena bioscience	Cat# NU-835-BIO14-S
dCTP (100mM)	Invitrogen	Cat# 10217016
dGTP (100mM)	Invitrogen	Cat# 10218014
dTTP (100mM)	Invitrogen	Cat# 10219012
DNA Polymerase Ⅰ, Large (Klenow) Fragment	New England Biolabs	Cat# M0210L
T4 DNA Ligase Reaction buffer	New England Biolabs	Cat# B0202S
T4 DNA Ligase	New England Biolabs	Cat# M0202S
Dynabeads™ MyOne™ Streptavidin C1	Invitrogen	Cat# 65001
e-Myco™ Mycoplasma PCR Detection kit (ver. 2.0)	iNtRON	Cat# 25235
FuGENE HD® Transfection Reagent	Promega	Cat# 2311
G418 disulfate salt	Sigma	Cat# A1720
Hygromycin B from *Streptomyces hygroscopicus*	Sigma	Cat# H3274
Blasticidin	InvivoGen	Cat# ant-bl-05
Indole-3-acetic acid sodium salt	Sigma	Cat# I5148
Propidium iodide solution	Sigma	Cat# P4864
Phenol:Chloroform:Isoamyl Alcohol	Sigma	Cat# P3803
Recombinant DNA		
pMK289 (mAID-mClover-NeoR)	Addgene	Cat# 72827
pMK290 (mAID-mClover-Hygro)	Addgene	Cat# 72828
pSpCas9(BB)-2A-Puro (PX459) V2.0	Addgene	Cat# 62988
pX330-U6-Chimeric_BB-CBh-hSpCas9	Addgene	Cat# 42230
pTK600	Addgene	Cat# 114696
pDendra2-C	Clontech	Cat# 632546
pUC19	Addgene	Cat# 50005
Materials for imaging		
35mm glass bottom dish	Cellvis	Cat# D35-25-1.5-N
ECLIPSE Ti2-E main body	Nikon	Cat# MEA54000
OBIS 405 nm LX 50 mW	Coherent	Cat# 1284369
OBIS 561 nm LS 150 mW	Coherent	Cat# 1280720
OBIS 640 nm LX 100 mW	Coherent	Cat# 1185055
Software and Algorithms		
MTT	Serge et al., 2008	https://github.com/cisselab/qSR
qSR	Andrews et al., 2018	https://github.com/cisselab/qSR
HaMMy	Mckinney et al., 2006	http://ha.med.jhmi.edu/resources/#1464200861600-0fad9996-bfd4
Hic-pro v2.11.4	Servant et al., 2015	https://github.com/nservant/HiC-Pro
coolpup.py v0.9.5	Flyamer et al., 2020	https://github.com/open2c/coolpuppy
Juicer tools v1.22.01	Durand et al., 2016	https://github.com/aidenlab/juicer/wiki/Juicer-Tools-Quick-Start
HiCExplorer v3.4.3	Ramirez et al., 2018	https://hicexplorer.readthedocs.io/en/latest
Fit-hichip v8.0	Bhattacharyya et al., 2018	https://github.com/ay-lab/FitHiChIP
STAR v2.6.0a	Dobin et al., 2013	https://github.com/alexdobin/STAR

RSEM v.1.2.31	Li and Dewey, 2011	https://deweylab.github.io/RSEM/
DESeq2 v1.26.0	Love et al., 2014	https://doi.org/10.18129/B9.bioc.DESeq2
trim_galore v0.6.4	Babraham Bioinformatics	https://github.com/FelixKrueger/TrimGalore
bwa v0.7.17	Li an Durbin, 2010	https://github.com/lh3/bwa
SAMtools v1.9	Li et al., 2009	http://samtools.sourceforge.net
Picard v2.18.23	Broad Institute	https://github.com/broadinstitute/picard
deeptools v3.4.3	Ramírez et al., 2016	https://github.com/deeptools/deepTools/
MACS2 v2.2.7.1	Zhang et al., 2008	https://github.com/taoliu/MACS
3DChromatin_ReplicateQC	Yardminci et al., 2017	https://github.com/kundajelab/3DChromatin_ReplicateQC
FlowJo v10.5.3	FlowJo LLC	https://www.flowjo.com/
GraphPad Prism v5.03	GraphPad Software Inc.	https://www.graphpad.com/
cooltools v0.3.2	Venev et al. 2019	https://github.com/open2c/cooltools
Fan-c v0.9.10	Kruse et al., 2020	https://github.com/vaquerizaslab/fanc